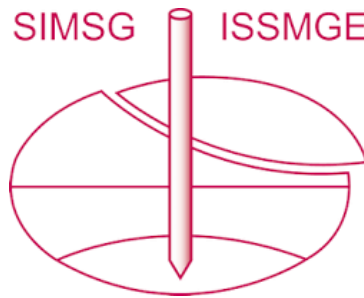


INTERNATIONAL SOCIETY FOR SOIL MECHANICS AND GEOTECHNICAL ENGINEERING



This paper was downloaded from the Online Library of the International Society for Soil Mechanics and Geotechnical Engineering (ISSMGE). The library is available here:

<https://www.issmge.org/publications/online-library>

This is an open-access database that archives thousands of papers published under the Auspices of the ISSMGE and maintained by the Innovation and Development Committee of ISSMGE.

The paper was published in the proceedings of the 20th International Conference on Soil Mechanics and Geotechnical Engineering and was edited by Mizanur Rahman and Mark Jaksa. The conference was held from May 1st to May 5th 2022 in Sydney, Australia.

An advanced constitutive model for silts and clays: a PLAXIS implementation of PM4Silt

Un modèle constitutif avancé pour les limons et les argiles: une implémentation PLAXIS de PM4Silt

Ilaria Del Brocco, Sandro Brasile, Xiaoyao Yang & Gregor Vilhar

Geotechnical research, Plaxis B.V., A Bentley System Company, Netherlands, Ilaria.delbrocco@bentley.com

Ronald B.J. Brinkgreve

Geo-engineering section, Faculty of Civil Engineering & Geo-sciences, Delft University of Technology, Netherlands

ABSTRACT: Many constitutive models are nowadays available to simulate the mechanical behaviour of clays under different loading conditions. For geotechnical engineering applications in a soil dynamics context, the PM4Silt model, as proposed by Boulanger & Ziotopoulou (2018), can simulate the cyclic behaviour of low-plasticity silts and clays. Formulated in a bounding surface plasticity framework, this model adapts the capabilities of a previous model suited for sands and non-plastic silts, i.e. PM4Sand, and enables to simulate more clay-like soil behaviour. In this paper, published calibrations for silts with different plasticity properties are employed to simulate the experimental results of monotonic and cyclic undrained DSS test with the purpose to comment on the effect of some key parameters, including the initial stress ratio K_0 and the bounding surface parameter $\eta^{b,wet}$. Numerical simulations are performed with the finite element implementation of PM4Silt in PLAXIS. Besides the two original methods to define undrained shear strength (based on S_u and $S_{u,ratio}$), a third method is proposed here based on the SHANSEP approach. The application of the model in view of the key parameters is demonstrated by means of a practical example.

RÉSUMÉ : De nombreux modèles de comportement sont aujourd'hui disponibles pour simuler le comportement mécanique des argiles sous différentes conditions de chargement. Pour les applications d'ingénierie géotechnique dans un contexte de dynamique des sols, le modèle PM4Silt, tel que proposé par Boulanger & Ziotopoulou (2018), peut simuler le comportement cyclique des limons et argiles à faible plasticité. Formulé dans un cadre de plasticité de surface englobante, ce modèle adapte les capacités d'un modèle précédent adapté aux sables et aux limons non plastiques, i.e. PM4Sand, et permet de simuler un comportement de sol plus argileux. Dans cet article, des étalonnages publiés pour des limons avec différentes propriétés de plasticité sont utilisés pour simuler les résultats expérimentaux du test DSS non drainé monotone et cyclique dans le but de commenter l'effet de certains paramètres clés, y compris le rapport de contrainte initial K_0 et le paramètre de surface englobante $\eta^{b,wet}$. Des simulations numériques sont réalisées avec l'implémentation par éléments finis de PM4Silt dans PLAXIS. Outre les deux méthodes originales pour définir la résistance au cisaillement non drainé (basées sur S_u et $S_{u,ratio}$), une troisième méthode est proposée ici basée sur l'approche SHANSEP.

KEYWORDS: PM4Silt, cyclic softening, SHANSEP, sensitive clays

1 INTRODUCTION

The seismic performance of civil and geotechnical structures significantly depends on the undrained cyclic behavior of soils. In both fine and coarse-grained soils, the build-up of high excess pore water pressures and shear strain levels can develop during earthquakes, but the loss of undrained strength is something typical for non-plastic soils (and quick clays). In nonstructured clays and low plasticity silts, strong earthquakes can still induce high levels of shear strains due to occurrence of cyclic softening (Boulanger & Idriss, 2007). Several cases have been documented in the last decades involving damage to buildings or geotechnical structures due to the dynamic response of fine-grained soils (Boulanger & Idriss 2004, 2007, Boulanger, 2019).

The PM4Silt constitutive model (Boulanger & Ziotopoulou, 2018) has been formulated to simulate the undrained cyclic loading response of low plasticity fine-grained soils. Unlike its predecessor PM4Sand (Boulanger & Ziotopoulou, 2018), PM4Silt includes features aimed to capture the undrained cyclic loading behaviour which is more typical for clay-like soils. Interestingly, PM4Silt has been recently used to simulate the mechanical response of sensitive clays as well (Kiernan & Montgomery 2020, Oathes & Boulanger, 2020). This advanced constitutive model is applicable in practical engineering (as PM4Sand) because it can be calibrated using primarily the results of in situ tests, and for a significant part of the numerous parameters default values are proposed which simplifies the calibration process.

Among the three primary parameters, as a minimum that must be calibrated, there is the undrained shear strength at critical state, $S_{u,cs}$, or alternatively $S_{u,ratio,cs}$ which is the undrained strength normalized over the current vertical effective stress. Except for quick clays and strongly cemented soils, the (normalized) undrained shear strength depends on the stress history of the deposit and its intrinsic properties.

Recently, the PM4Silt model has been implemented in the PLAXIS finite element software and validated in comparison with the original implementation of the model (Yang, 2020; Bentley, 2021). Herein, a new approach has been incorporated aimed at initializing $S_{u,cs}$ in each stress point individually by estimating $S_{u,cs}$ using the Stress History And Normalized Soil Engineering Properties concept (SHANSEP; Ladd & Foott, 1974) with parameters α and m , the overconsolidation ratio OCR, and the effective stress at the start of the dynamic analysis. In numerical simulations, the initial state of a dynamic analysis can be the result of multiple preceding static phases. PLAXIS keeps track of the maximum principal effective stress reached in each stress point during all phases and provides a distribution of the OCR in the entire soil domain. Multistage analyses are very useful, in general, to obtain a realistic effective stress distribution with proper stress ratios and static shear stresses, in contrast to single phase gravity loading or K_0 generated initial stress fields. This is particularly relevant in the case of slopes or earth dams. The presentation of the SHANSEP approach to initialize the undrained shear strength in the PM4Silt model is the first goal of this paper.

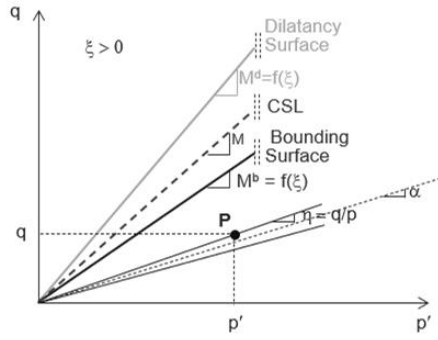


Figure 1. Representation of bounding and dilatancy stress ratios for a given positive value of the state parameter, ξ .

The second goal is to discuss the role of some key-parameters in view of a potential instability phenomenon which can have a considerable impact on the soil behaviour during seismic analyses. Specifically, the parameters affecting the bounding surface in relation to the initial stress state are discussed to provide further insight in this instability phenomenon. Moreover, a solution strategy is provided to properly use PM4Silt model in numerical earthquake simulations of practical applications.

2 SOME KEY ASPECTS OF THE PM4SILT MODEL

PM4Silt is a stress-ratio controlled, critical state compatible bounding surface model formulated on the framework of the PM4Sand constitutive model for plain strain applications. The out-of-plane stress component does not influence the plastic mechanism of the models. Therefore, the invariants of the effective stress tensor are defined as

$$p' = \frac{\sigma'_{xx} + \sigma'_{yy}}{2} \text{ and } q = 2\sqrt{\left(\frac{\sigma'_{xx} - \sigma'_{yy}}{2}\right)^2 + (\tau_{xy})^2} \quad (1)$$

PM4Silt requires the definition of 19 parameters grouped in two main categories: 3 primary and 16 secondary parameters. The primary parameters include: the dimensionless small strain stiffness constant G_0 , used in the elastic shear modulus definition; the contraction rate parameter h_{p0} , which strongly influences the cyclic resistance; and the undrained shear strength, $S_{u,cs}$ which replaces the relative density, D_r as used in PM4Sand. As an alternative to the input of $S_{u,cs}$, PM4Silt allows specifying the normalized strength ratio $S_{u,ratio,cs}$, instead. The formulation of the model and the role of all parameters are extensively described in Boulanger & Ziotopoulou, 2018, 2019.

In contrast to what is common in other bounding surface plasticity models, PM4Silt derives the initial value of the state parameter,

$$\xi_0 = e_0 - e_{cs} \quad (2)$$

implicitly from the specified undrained shear strength, where e_0 is the initial void ratio, an input parameter, and e_{cs} is the void ratio on the critical state line (CSL) for the initial mean effective stress, p'_0 . The CSL is only partially defined through the input parameters, but the intercept Γ can be derived from

$$\Gamma = e_0 + \lambda \cdot \ln \left[101.3 \left(\frac{p'_{cs}}{p_{atm}} \right) \right] \quad (3)$$

where

$$p'_{cs} = 2 S_{u,cs} / M \quad (4)$$

and M is the inclination of the CSL in (p', q) stress space.

The critical state void ratio e_{cs} is a function of the initial mean effective stress p'_0 and can be defined from

$$e_{cs} = \Gamma - \lambda \cdot \ln \left[101.3 \left(\frac{p'_0}{p_{atm}} \right) \right] \quad (5)$$

Now, the initial value of the state parameter, ξ_0 can be calculated by substituting equations 3 to 5 in 2.

A first approach to the calibration of parameters can be that of using $S_{u,cs}$ as a direct input. In such a case, a unique CSL as well as a constant undrained strength $S_{u,cs}$ is considered for the whole domain. Since the initial void ratio, e_0 , is also constant in the whole domain, this would imply that different stress points characterized by different mean effective stress levels will have a different initial state parameter ξ_0 .

Conversely, when $S_{u,ratio,cs}$ is used in lieu of $S_{u,cs}$ as the primary input parameter, e_{cs} is the same for all the stress points where K_0 is the same because the undrained strength at critical state in Eq. 4 is computed in every stress point as a function of the initial vertical effective stress, σ'_{v0}

$$S_{u,cs} = S_{u,ratio,cs} \sigma'_{v0} \quad (6)$$

In this case, different stress points in the domain will have different undrained shear strengths, and consequently, different critical state lines but the same initial state parameter ξ_0 , by being the initial void ratio, e_0 , the same (= input parameter)

A second key aspect of PM4Silt is the specific definition of the bounding stress ratio M^b for states looser than the critical state, i.e.

$$M^b = M \exp \left(-n^{b,wet} \frac{\xi}{\lambda} \right) \text{ for } \xi > 0 \quad (7)$$

in which the model parameter $n^{b,wet}$ controls the evolution of the bounding surface inclination M^b as a function of the state parameter, ξ (Figure 1). The role of this parameter can be appreciated from Figure 3 where the bounding and dilatancy loci are plotted for different values of the state parameter, ξ_0 and a single value of the void ratio, e_0 . In particular, the parameter $n^{b,wet}$ influences the mechanical response predicted in monotonic tests (Figure 4), specifically regulating the peak shear strength and the apparent softening in DSS test simulations. For $n^{b,wet} = 1$ the bounding locus is flat (Figure 3) and the stress-strain response does not show a peak (Figure 4), whereas for $n^{b,wet} < 1$ the bounding surface becomes steeper. This allows simulating the mechanical response of sensitive clays or sand-like behavior including a peak undrained strength and apparent softening behaviour (Boulanger & Ziotopoulou, 2019, Kieran & Montgomery, 2020, Oathes & Boulanger, 2020).

Figure 3 also shows that for $n^{b,wet} \cong 1$ or small undrained strength at critical state, the initial stress ratio (represented by the narrow yield surface) can be higher than the bounding stress ratio, leading to an unrealistic model response. This demonstrates the importance of accounting for the initial stress state during the calibration of the parameters $n^{b,wet}$ and $S_{u,cs}$ or $S_{u,ratio,cs}$.

3 SHANSEP APPROACH IN PLAXIS

In addition to the two basic methods to define the critical state undrained shear strength in the PM4Silt model (direct input of $S_{u,cs}$ or input of the normalized shear strength ratio, $S_{u,ratio,cs}$), a new approach is proposed here using a slightly modified version of the SHANSEP equation (Ladd & Foott, 1974), as implemented in some PLAXIS constitutive models (Panagoulas et al., 2016). In the modified SHANSEP equation adopted here, the undrained shear strength is initialized, as

$$S_{u,cs} = \sigma'_1 \alpha (OCR)^m \quad (8)$$

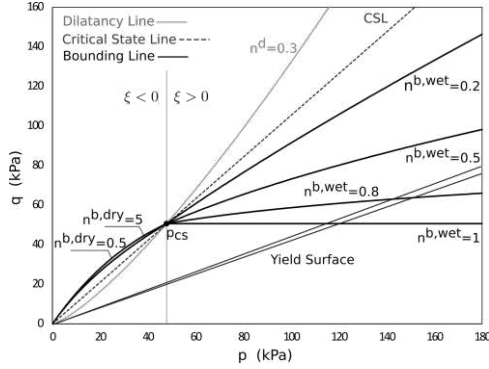


Figure 3. Influence of parameter $n^{b,wet}$ on the effective trend of the BS on the wet-side.

in which σ'_1 is the major principal effective stress, OCR is the over-consolidation ratio defined as $OCR = \sigma'_{1,max}/\sigma'_1$, α is the normalized undrained shear strength ratio in a state of normal consolidation (in this case normalized by the major principal effective stress), and m is the power accounting for the OCR-dependency of the shear strength ratio. Note that the difference between the formulation adopted here and the original SHANSEP formulation is the normalization based on major principal effective stress instead of vertical effective stress. This formulation has some advantages in the case of slopes, dams and embankments involving rotation of the major principal effective stress compared to the use of vertical effective stress.

The $S_{u,ratio}$ is then calculated, based on the definition used in PM4Silt

$$S_{u,ratio,cs} = \frac{S_{u,cs}}{\sigma'_{v0}} \quad (9)$$

and subsequently used to compute some of the secondary parameters for which a standard formula can be used. The mean effective stress at critical state is therefore unaffected by the $S_{u,ratio}$ as defined in Eq. 4. For details, reference is made to Boulanger & Ziotopoulou, 2018.

The advantage of this third option to introduce the undrained shear strength using the SHANSEP formula is that the stress history is explicitly taken into account, i.e. the influence of overconsolidation and vertical effective stress (or major principal effective stress), which may differ at different locations in the same soil strata.

The correct definition of the initial state of a dynamic analysis is crucial to obtain reliable results. Advanced 'static' constitutive models can be used in preceding calculation phases to accurately build up the initial state of stress; for example, multi-stage construction of a dam. During each preliminary calculation step and phase, the maximum major principal effective stress ever experienced in a stress point, $\sigma'_{1,max}$, is memorized and passed on to the next step and phase, for each stress point individually.

After the preceding phases, a 'switch' is made to the PM4Silt model in the subsequent dynamic analysis. At this moment, the SHANSEP equation is used in each stress point to initialize the undrained shear strength, thereby adopting the stress level and stress history (i.e. OCR) from all previous phases.

4 INITIAL CONDITIONS AND PARAMETERS CALIBRATION

The basic idea of PM4Silt is to provide, as input parameters, quantities that can be measured directly, and then, by considering principles of the critical state soil mechanics and properties of clay-like materials (i.e. S_u or $S_{u,ratio}$), to derive the state parameter ξ and other parameters that automatically reproduce

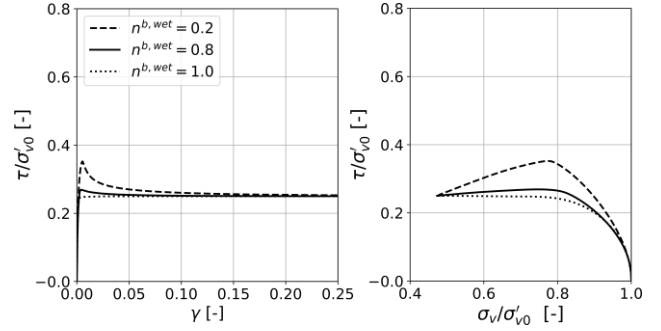


Figure 4. Influence of parameter $n^{b,wet}$ on the results of monotonic DSS tests performed with $S_{u,ratio} = 0.25$ and $G_0 = 588$, $h_{p0} = 20$.

the measured resistance. This philosophy allows overcoming issues related to the heterogeneity of in situ soils, which makes the model attractive (as PM4Sand) for practical engineering applications. Consequently, some input parameters become related to the initial state, as already explained in Section 2.

To explore a possible strategy for calibrating the model parameters, to be used in numerical analyses of boundary value problems, taking into account the aforementioned relationships between some of the parameters and the initial stress, the results of monotonic and cyclic undrained DSS tests, as shown in Figures 5 and 6, are considered.

The results in Figures 5 and 6 are obtained from single stress point simulations using the following parameters in common: $S_{u,ratio,cs} = 0.145$, $G_0 = 736$, $h_{p0} = 2.2$, $e_0 = 0.61$, $\lambda = 0.07$, $\varphi_{cs} = 32^\circ$, $r_{u,max} = 0.99$, $C_z = 150$, $C_\epsilon = 1$. These are the result of an initial parameter calibration, as reported by Boulanger & Ziotopoulou, 2018. Since the parameters h_{p0} , $r_{u,max}$, C_z and C_ϵ mainly influence the results of cyclic tests, and $S_{u,ratio,cs}$, G_0 , φ_{cs} and λ can be obtained from in situ tests or laboratory tests, attention will be paid to the initial stress ratio assumed in the DSS tests to find the most suitable value of the other parameters. The procedure for calibrating PM4Silt (Boulanger & Wijewickreme, 2019) requires adjusting $n^{b,wet}$ (starting with the default value) to capture the peak shear stress observed in monotonic UDSS tests (Figure 4).

Before calibration of $n^{b,wet}$, attention must be paid to K_0 because it can influence the range of admissible values for $n^{b,wet}$. K_0 can also be incompatible with the aim of simulating a ductile monotonic undrained response.

When measurements are not available, an estimate of K_0 could be based upon the well-known empirical correlation

$$K_0 \cong (1 - \sin(\varphi_{cv})) OCR^{\sin(\varphi_{cv})} \quad (10)$$

Given the initial vertical effective stress in a numerical simulation of a practical application or lab test (such as the DSS test), the assumed K_0 value influences the initial mobilized shear strength that must be below the peak shear strength, $S_{u,max}$ to form a valid stress state in PM4Silt. The point is that $S_{u,max}$ cannot be easily determined based on the input parameters.

Taking $S_{u,cs}$ (or $S_{u,ratio,cs} \sigma'_{v0}$) as a conservative estimate of $S_{u,max}$, it can be argued that for

$$K_0 > 1 - 2 S_{u,ratio,cs} \quad (11)$$

the initial stress state is always valid. However, the violation of the condition in Eq. 11 does not necessarily mean that the stress state is invalid, since $S_{u,max}/\sigma'_{v0}$ may be higher than $S_{u,ratio,cs}$, as depicted in Figure 4. This is where the $n^{b,wet}$ parameter comes into play.

When Eq. 11 holds, any positive value for $n^{b,wet} < 1$ can be assumed and $S_{u,max}/\sigma'_{v0} \geq S_{u,ratio,cs}$ can be simulated.

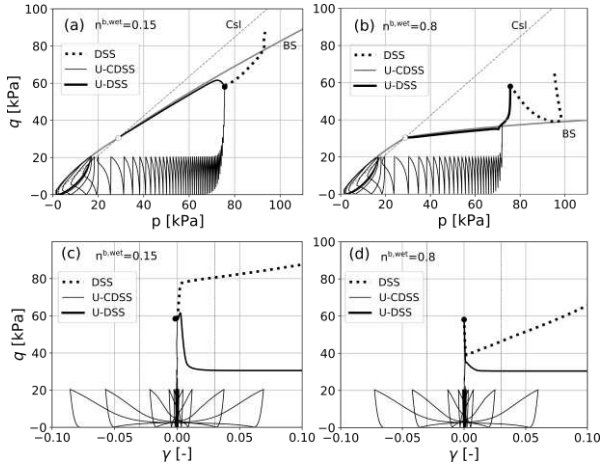


Figure 5. Influence of $n^{b,wet}$ in single stress-point simulation. (a) (b) on the BS and the effective stress paths. (c) (d) On the stress-strain relationships in terms of $\gamma_{xy} - q$. The initial stress, (black symbol).

On the hand, if Eq. 11 is violated, two scenarios are possible.

If it is considered realistic that $q_0 \geq 2S_{u,cs}$ (since $S_{u,max} > S_{u,cs}$, as for sensitive clays), $n^{b,wet}$ must be calibrated first to guarantee a valid initialization of the bounding surface and also to capture the $S_{u,max}$ observed in the experimental tests. If it is not realistic (because the material exhibits $S_{u,max} = S_{u,cs}$ as for non-cemented clays), $n^{b,wet}$ must be considered as fixed. In this case, either $S_{u,cs}$ or K_0 should be increased to guarantee Eq. 11.

In all cases, a valid initialization is achieved if $\eta_0 = q_0/p'_0 < M_0^b$. In Figure 5ab the initial conditions of the test are $K_0 = 0.44$ and $\sigma'_{v0} = 105 \text{ kPa}$. The assumed K_0 of 0.44 violates Eq. 11, because, for $S_{u,ratio} = 0.145$, the limit is $K_0 = 0.71$ and consequently, for the initial state (black dot) $q_0 > 2S_{u,cs}$. Taking the default value $n^{b,wet} = 0.8$ (as done in Figure 5b), the initial state would also lie above the bounding surface BS ($\eta_0 > M_0^b$). Such an initial configuration involves an incompatible stress state and is therefore considered invalid.

In the first step of both the drained and undrained monotonic DSS tests in Figure 5bd the resistance is not sufficient to sustain the initial q_0 , hence stress reduction must occur. In the UDSS, the effective stress path (solid black line) adapts to the bounding surface and follows its way to the critical state line (CSL). In the drained DSS test (dashed line) although the resistance at critical state is higher than the initial q_0 , a deviatoric stress reduction is still experienced by the soil. Consequently, in boundary value problems, this initial stress decrease can lead to failure in the drained static analysis or at the beginning of the undrained analysis. Figure 5a shows the effective stress path in (p', q) -space using $n^{b,wet} = 0.15$. This leads to an initial stress state below the bounding surface. Unlike the previous case, the peak undrained shear strength is higher than the initial q_0 and, although an unstable undrained monotonic response is simulated, the stress ratio keeps increasing even after the mobilization of $S_{u,max}$. Positive deviatoric hardening also occurs during the drained test (dashed line). Such predictions are more in agreement with typical results provided by other stress ratio-controlled bounding surface models for a positive initial state parameter.

Calibrations leading to mechanical responses similar as obtained with $n^{b,wet} = 0.15$ have been found by Kiernan & Montgomery 2020 simulating the response of a sensitive clay, but they could also occur in silts with a more sand-like behavior. For these cases, the need for $n^{b,wet} < 1$ to guarantee $\eta_0 < M_0^b$ in case Eq. 11 is violated, does not really conflict with the experimental soil behavior, since such soils generally exhibit $S_{u,max} > S_{u,cs}$ and a compromise is easily found. For non-structured clays, it is unlikely that the initial state can be higher

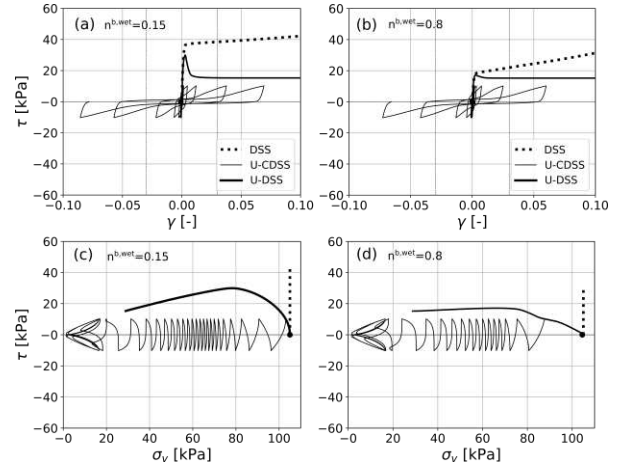


Figure 6. Influence of $n^{b,wet}$ in single stress-point simulation. (a) (b) on the stress-strain relationships in terms of $\gamma_{xy} - \tau_{xy}$. (c) (d) On the stress paths in the $\sigma'_v - \tau_{xy}$. The initial stress, (black symbol).

than the undrained strength because a relatively ductile response is expected. Therefore, the reduction of $n^{b,wet}$ would create a side effect of obtaining an $S_{u,max}$ that exceeds the experimental soil behavior. As anticipated, in these situations either $S_{u,ratio,cs}$ is not high enough or K_0 must be forced to respect Eq. 11.

The strategy to calibrate the input parameters in accordance with the initial state is:

- use Eq. 11 to detect if $q_0 > q_{cs}$. For non-lithostatic initial conditions, where τ_{xy} is non-zero, Eq. 11 can be used assuming $K_0 = \sigma'_3/\sigma'_1$ where σ'_1 and σ'_3 are major and minor principal effective stresses.
- if Eq. 11 is violated and condition $q_0 > q_{cs}$ considered realistic, it is suggested to perform monotonic DSS test simulations, even when experimental test results are not available, with the principal aim of verifying the compatibility of the initial state with the bounding surface. The occurrence of $\eta_0 > M_0^b$ can be detected without the need to create a (p', q) stress plot, but just by examining the trend of $\sigma'_v - \tau_{xy}$. The results of the monotonic UDSS tests are plotted in Figure 6 in terms of $\sigma'_v - \tau_{xy}$ and $\gamma_{xy} - \tau_{xy}$. An irregular 'curvature' of the monotonic stress path can be seen in the case of $n^{b,wet} = 0.8$. Notice that in the drained tests, the occurrence of the temporary deviatoric shear stress drop is harder to be deduced without explicitly examining the trend in the q - p' space. The $\gamma_{xy} - \tau_{xy}$ and $\sigma'_v - \tau_{xy}$ results look very similar. Another reason why the monotonic UDSS test is useful is that in a U-CDSS test the effect is barely visible. If the amplitude of $\Delta\tau_{xy}$ is low, the curvature of $\sigma'_v - \tau_{xy}$ is not noticeable. In the $\sigma'_v - \tau_{xy}$ space (Figure 6), the influence of $n^{b,wet}$ reflects only in the number of cycles required to reach cyclic failure.

The occurrence of $\eta_0 > M_0^b$ is automatically detected in the current implementation of PM4Silt in PLAXIS and the stress state is corrected to restore consistency with the bounding surface.

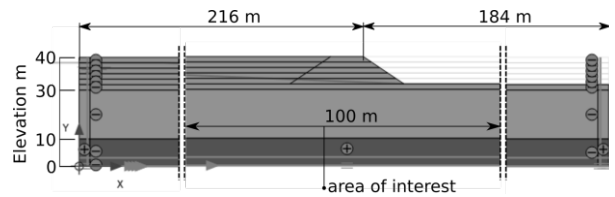


Figure 7. PLAXIS model of the slope.

5 USE OF PM4SILT IN BOUNDARY VALUE PROBLEMS

The initialization of the back-stress ratio, α_0 , and the state parameter, ξ_0 requires an initial effective stress distribution, therefore, in general boundary value problems, before using PM4Silt, at least an equilibrium phase is performed with a different constitutive model.

The initial stress state of a dynamic analysis should be, equilibrated, but also realistic, and as explained before, compatible with the calibrated parameters. Unrealistic aspects can be related to, for instance, the K_0 distribution. In numerical modeling of dams or slopes often multi-stage static analyses are performed to reach a realistic distribution of the effective stress.

The simulations shown in this paragraph pertain to the dynamic analyses of the model in Figure 7. The simple model involves two static stages to be executed prior to the dynamic analysis with PM4Silt with the purpose of demonstrating the strategy to define a reliable initial state and the change of constitutive model from the static to the dynamic analysis.

The stratigraphy of the slope is formed by a fine-grained soil delimited by an elastic bedrock with properties $E = 3E^6 \text{ kPa}$, $\nu = 0.2$, $\gamma_{sat} = \gamma_{unsat} = 20 \text{ kN/m}^3$ and $e_0 = 0.5$. The fine-grained soil is initially modelled by the Hardening Soil (HS) and later switched to PM4Silt. In both cases $\gamma_{sat} = 18.43 \text{ kN/m}^3$, $\gamma_{unsat} = 13.7 \text{ kN/m}^3$ and $e_0 = 0.9$. The inclination of the slope is 1:1.5. The extent of the model is 420 m to limit the influence of the boundary conditions on the results of the dynamic analysis. Figure 7 shows the area of interest over which results are shown in the next paragraphs. The area excludes the elastic layer because only PM4Silt state variables are considered.

The initial state of the slope is reached through an excavation performed in multiple stages. After applying initial lithostatic conditions five drained excavation phases are performed. Purely frictional resistance is considered for the HS model, the same as in PM4Silt, (Table 1) and a dilatancy angle at failure $\psi = 0^\circ$. Furthermore $E_{ur}^{ref} = 150000 \text{ kPa}$, $p_{ref} = 100 \text{ kPa}$, $\nu = 0.2$ and $m = 1$ are chosen to obtain, at the end of the static analyses, a distribution of the stiffness, G close to the one of PM4Silt and scaled to 70% to account for the different strain levels involved in static and dynamic analyses. $E_{50}^{ref} = E_{oed}^{ref} = 10000 \text{ kPa}$ are assumed, which are typical values for fine grained soils. The hypothesis is that the soil is normally consolidated with $K_0^{nc} = 0.4264$, in accordance with Eq. 10. The permeability of the bedrock and the soil are respectively $k_x = k_y = 10^{-7} \text{ m/s}$ and $k_x = k_y = 10^{-6} \text{ m/s}$. The water level, initially two meters below the ground surface in lithostatic conditions, is progressively lowered inside the excavation during the excavation stages and the free surface-steady flow is updated at the beginning of each plastic equilibrium phase to simulate a drained excavation process. Although this example may not be fully realistic, it allows to schematically take the presence of water and the development of over-consolidation under the excavation into account, demonstrating the effect of OCR on the distribution of the normalized undrained strength according to the SHANSEP approach.

Figure 8 shows the distribution of OCR. The $S_{u,ratio}$ back-calculated based on the vertical effective stress is shown in Figure 9, together with the contours of $\alpha_{static} = \tau_{xy}/\sigma'_v$. In the zones where OCR=1 and the level of shear stress is low, note that $S_{u,ratio} \cong \alpha = 0.25$ (parameter set M1 in Table 1). In zones where $S_{u,ratio} \leq 0.34$, ξ_0 shows positive values. The indicator BCI, included in PLAXIS with the PM4Silt state variables, is set to 1 if $\eta_0 > M_0^b$ and therefore allows to visualize areas in which

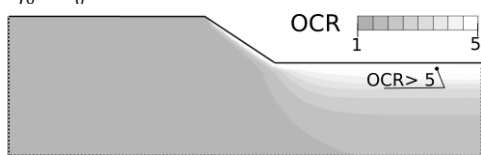


Figure 8. OCR contours at the end of the drained excavation.

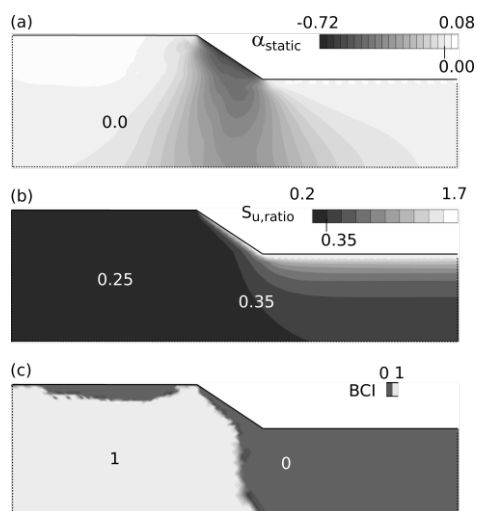


Figure 9 Contours of: (a) the static shear stress ratio. (b) $S_{u,ratio}$ calculated based on S_u provided by the SHANSEP formula with the parameter set M1 (c) Bounding Correction Indicator for an hypothetical $n^{b,wet} = 1$ in combination with $S_{u,ratio}$ of Figure (b).

the condition was violated (and the stress state was corrected). Attention here is put on the zones where BCI is 1 and ξ_0 is positive to verify the adequacy of $n^{b,wet}$.

$n^{b,wet} = 0.15$ is assumed for the first simulation (parameter set M1 in Table 1), which allows the initial stress distribution to be compatible with the BS, for the assigned $S_{u,ratio}$ and the initial stress state. After the switch to PM4Silt, in whole domain BCI=1 indicating $\eta_0 < M_0^b$, which is good.

However, considering that the soil is more ductile by assuming $n^{b,wet} = 1.0$ instead of 0.15, in the area indicated by BCI=1 in Figure 9c, $\eta_0 > M_0^b$. This means that in that zone, $q_0 > q_{cs}$, and therefore a potential instability may occur during the earthquake. It is interesting to see that for $n^{b,wet} = 1.0$, BCI=1 occurs in an area where $\alpha_{static} = \tau_{xy}/\sigma'_{v0}$ is quite high, and this shear stress can lead to failure during the earthquake. This simple check can be used to identify areas of potential unstable response.

In case of lack of convergence of the static equilibrium that follows after the switch to PM4Silt, plotting the BCI distribution, with the calibrated $n^{b,wet}$ can be useful because, if BCI=1 in a wide area of the model, the cause of failure can be that the calibrated $n^{b,wet}$ does not match the initial effective stress and therefore, either $S_{u,ratio}$ or $n^{b,wet}$ or K_c has to be adjusted.

The flat trend of the BS on the wet-side allows to simulate ductile undrained response but restricts the range of admissible

Table 3. PM4Silt.

Primary parameters	M1	M2
G_0 (-)	588	588
h_{p0} (-)	40	40
Customized secondary		
n_G (-)	0.6	0.6
e_0 (-)	0.9	0.9
φ_{cv} (°)	36	36
$n^{b,wet}$ (-)	0.15	1.0
Parameters SHANSEP for $S_{u,cs}$		
α (-)	0.25	0.37
m (-)	0.91	0.91

initial stress ratios. When the shape of the BS on the wet-side is closer to the CSL, (as it usually is in models for sands), to guarantee the equilibrium after the switch of model, K_0 must

range between K_a and K_p . When $n^{b,wet}$ is imposed with the intention of simulating a ductile response, K_0 should be forced to stay in the range that allows to have $\eta_0 < M_0^b$ even though this would not be so realistic.

As an additional example case, a second parameter set is considered (M2 in Table 1), in which a higher $S_{u,ratio}$ has been assigned through a higher α -value, to allow for the convergence of the static equilibrium with $n^{b,wet} = 1$ while maintaining the initial stress state. The choice could have been to force the initial stress ratio to lie inside the range required for compatibility with the BS, but in this case the shear resistance was increased. Although assigning a higher resistance for the same stiffness parameters may not be realistic, the focus is on ways to ensure the compatibility of the initial state. The other parameters are quite similar to the basic calibration proposed by Boulanger & Ziotopoulou, 2018. The contraction rate parameter is set to $h_{p0} = 40$ only to reduce the rate of p' reduction. Note that, the scenario in which M2 is used represents a case to have $q_0 > q_{cs}$, would be not realistic due to $n^{b,wet} = 1$.

Free-field boundary conditions are applied on the sides of the model. To limit the distortion of the mesh, after the switch to the dynamic phase, a linear elastic material, with a drained response, is assigned to the elements located at the top of the mesh sides. The extent of the mesh is sufficient to exclude any influence of the boundary conditions on the results. A compliant base boundary condition is assigned at the model base, to minimize the development of noise in the model due to wave reflections. The time-history of horizontal acceleration shown in in Bentley, 2021 (Figures 20 to 22) is applied at the base of the model. The input motion is a recorded time series scaled (with a coefficient 2) to $a_{max} = 0.35g$ and low pass filtered at $f = 14\text{Hz}$. Drift correction option has been applied in the analyses.

The results of the two undrained dynamic analyses performed with calibrations M1 and M2 are shown in Figures 10.

The distribution of the extreme values of the maximum deviatoric shear strain, $\epsilon_{s,max}$ at the end of the earthquake simulation is shown in Figures 10a and b for the two cases.

Although in both figures the maximum deviatoric shear strain are similar in a significant part of the model ($\epsilon_{s,max} < 5\%$), in Figure 10a the strain has localized in a narrow band, which starts to develop after 10 s. Figure 10a can be interpreted as the result of a failure mechanism (this result seems in agreement with Kieran & Montgomery, 2020, with calibrations characterized by very small $S_{u,ratio}$ and $n^{b,wet}$, aimed to simulate sensitive clays).

In Figure 10b, on the other end, the higher maximum shear strains are around 12% and appear more diffuse. High damage levels but an unclear mechanism is obtained in this case. The considerable difference between the results obtained by the two parameter sets indicates the capability of PM4Silt to capture different kinds of responses.

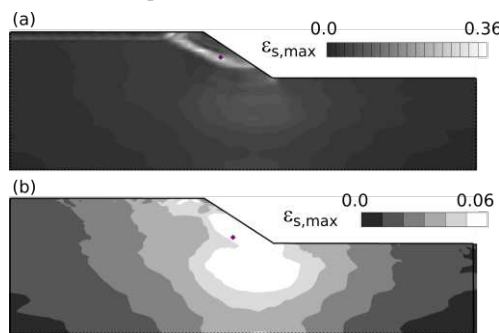


Figure 10. Maximum deviatoric shear strain reached at the end of the analyses ($t = 60$ s). (a) Calibration M1. (b) Calibration M2.

It is worth underlining that the change in parameters changes the initial ratio between q_0 and q_{cs} , which seems the main cause of the difference in results. Indeed, while $n^{b,wet} < 1$ only

influences the possibility that a peak q can occur (that depends also on the intensity of the input motion), the mobilization of q_{max} can lead to different phenomena based on the initial state of the soil.

6 CONCLUSIONS

In this paper we presented a new implementation of the PM4Silt constitutive model for cyclic loading behaviour and the associated stiffness and strength degradation in fine grained soils in the finite element program PLAXIS. Emphasis has been given to the initial stress state in relation to the choice of the model parameter $n^{b,wet}$. A strategy has been presented how $n^{b,wet}$ and other model parameters as well as the initial stress state, can be adapted to avoid an unstable and invalid model response. Moreover, a new way of determining the undrained shear strength in the model has been presented, based on a modified version of the SHANSEP equation. This method takes account of the distributed stress history prior to the dynamic analysis in which the PM4Silt model is used.

The application of the model and the relevance of the new way of introducing shear strength has been demonstrated by means of a practical example involving a slope, considering two different cases with parameter sets M1 and M2, representing different mechanical responses. The example also demonstrates the proposed way of detecting possible incompatibilities as well as the strategy of adapting model parameters in relation to the initial stress state. The obtained results are in accordance with the those which PM4Silt has been used previously to simulate a sensitive clay and a fine-grained soil with a clay-like response.

7 REFERENCES

- Bentley, 2021. PM4Silt – A silt plasticity model for earthquake engineering. User Manual. PLAXIS Connect Edition V21.00. Bentley Systems
- Boulanger R.W. and Idriss I.M., (2007). Evaluation of cyclic softening in silts and clays. Journal of Geotechnical and Geoenvironmental Engineering, 133(6), pp.641-652.
- Boulanger, R.W. and Wijewickreme, D., 2019, October. Calibration of a constitutive model for the cyclic loading response of Fraser River Delta Silt. In Earthquake Geotechnical Engineering for Protection and Development of Environment and Constructions: Proceedings of the 7th International Conference on Earthquake Geotechnical Engineering, (ICEGE 2019), June 17-20, 2019, Rome, Italy (p. 121). CRC Press.
- Boulanger, R.W. and Ziotopoulou, K., 2018. PM4Silt (Version 1): A silt plasticity model for earthquake engineering applications. Report No. UCD/CGM-18/01, Center for Geotechnical Modeling, Department of Civil and Environmental Engineering, University of California, Davis, CA
- Boulanger, R.W. and Ziotopoulou, K., 2019. A constitutive model for clays and plastic silts in plane-strain earthquake engineering applications. Soil Dynamics and Earthquake Engineering, 127, p.105832.
- Boulanger, R.W., 2019. Nonlinear Dynamic Analyses of Austrian Dam in the 1989 Loma Prieta Earthquake. Journal of Geotechnical and Geoenvironmental Engineering, 145(11), p.05019011.
- Kiernan M., Montgomery J., 2020. Numerical Simulations of Fourth Avenue Landslide Considering Cyclic Softening. J. Geotech. Geoenviron. Eng., 2020, 146(10): 04020099
- Oathes T.J., Boulanger R.W., 2020. Influence of Strain-Rate on localization and Strain-Softening in normally consolidated clays with varying strength profiles. Geo-Congress 2020 GSP 317, 247-255.
- Panagoulas S, Palmieri F., Brinkgreve R.B.J., 2016. PLAXIS – The SHANSEP MC model – User Manual. Delft: Plaxis bv.
- Yang X 2020. The cyclic behavior of low-plasticity silts and clays using the PM4silt model in PLAXIS 2D. MSc thesis. Delft University of Technology.